Available online at www.sciencedirect.com

ScienceDirect

Journal of Sound and Vibration 321 (2009) 572–589

JOURNAL OF SOUND AND VIBRATION

www.elsevier.com/locate/jsvi

Identification of linear time-varying mdof dynamic systems from forced excitation using Hilbert transform and EMD method

Z.Y. Shi[a], S.S. Law[b,*], X. Xu[a]

[a]*College of Aerospace Engineering, Nanjing University of Aeronautics and Astronautics, China*
[b]*Department of Civil and Structural Engineering, Hong Kong Polytechnic University, Hong Kong*

Received 6 July 2007; received in revised form 30 September 2008; accepted 4 October 2008
Handling Editor: L.G. Tham
Available online 20 November 2008

Abstract

An algorithm is developed for the identification of linear time-varying (LTV) multiple degrees-of-freedom systems. It is based on the Hilbert transform and the empirical mode decomposition with forced vibration response data. The proposed identification algorithm is applied to single degree-of-freedom and multi-degrees-of-freedom dynamic systems. Three ideal cases of LTV systems, with smoothly varying, abruptly varying and periodically varying stiffness and damping, are studied to illustrate the capability of the algorithm to track the variations of the system. Simulation results demonstrate the effectiveness and the robustness of the proposed identification algorithm, and the lack of complete orthogonality for any two intrinsic mode functions is one of the sources of error in the identification.

1. Introduction

The identification of linear time-varying (LTV) system has received increasing attention in recent years because most structures exhibit time-varying dynamic characteristics. The LTV models are more appropriate and better than the linear time-invariant (LTI) models for describing the instantaneous dynamic behaviors of systems [1]. The identification techniques of LTV have been successfully used to assess the condition of the system or to detect structural damage. Various identification techniques have been proposed using discrete-time state-space identification algorithms [2–5], wavelet transform theory [6–7], the adaptive tracking method [8–10] and Hilbert transform (HT) method [11–13].

In a previous work by the authors [13], an identification algorithm for LTV dynamic systems based on the Hilbert transformation and empirical mode decomposition (EMD), has been developed and verified with free vibration response data. Three ideal cases of single degree-of-freedom (sdof) and multiple degrees-of-freedom (mdof) time-varying systems, namely, the smoothly varying system, abruptly varying system and periodically varying system, are studied to demonstrate the identification process and its effectiveness.

*Corresponding author.
E-mail addresses: zyshi@nuaa.edu.cn (Z.Y. Shi), cesslaw@polyu.edu.hk (S.S. Law).

0022-460X/$ - see front matter
doi:10.1016/j.jsv.2008.10.005

In this paper we will use the HT and EMD to further develop the identification algorithm for the LTV system from the forced vibration response data. The paper is organized as follows. Section 2 introduces the basic theory of the EMD and its orthogonality. Section 3 develops the identification algorithm for the LTV mdof systems via forced vibration response data. Section 4 demonstrates the identification procedure with numerical examples and discusses the effectiveness and accuracy of the proposed method. Conclusions are presented in Section 5.

2. The EMD

One of the common approaches to study the time-varying dynamic properties of a system, such as the instantaneous frequency, is the HT [11–12]. In order to obtain meaningful instantaneous frequency, restrictive requirements have to be imposed on the data, i.e., the data should be an intrinsic mode function (IMF). The IMF is a function that satisfies two conditions: (1) in the whole range of data, the number of extrema and the number of zero crossing must either equal or differ at most by one and (2) at any point, the mean value of the envelope defined by the local maxima and the envelope defined by the local minima is zero. Unfortunately, most of the data are not IMFs, and that is why the HT cannot provide full description on the frequency content for data in general.

Huang et al. [1] have proposed a method of EMD to decompose a general signal into IMFs resulting in well-behaved HT. The procedure of EMD is (1) to identify all the local maxima and minima of the signal and to construct the upper and lower envelopes of the signal by cubic splines; (2) to compute the mean of upper and lower envelopes, and to subtract this mean from the original signal. These two steps are known as the sifting process; (3) to repeat the sifting process until the resulting signal satisfies the above two conditions for an IMF. This signal is then suitable for HT analysis and (4) to form a new signal by subtracting the IMF from the original signal, and repeat Steps 1–3 to obtain another IMF. The process is repeated until the residual signal becomes small and is less than a pre-determined value or the residual signal becomes a monotonic function.

For an n degrees-of-freedom system, n IMFs can be obtained after the sifting process. The original signal can be expressed as

$$y(t) = \sum_{j=1}^{n} y_j(t) + r(t) \tag{1}$$

in which ($y_j(t)$, $j = 1,2,\ldots,n$) are the IMFs of the original signal, and $r(t)$ is the residue, which is a monotonic function from which no more IMF can be extracted.

As discussed in Ref. [1], the orthogonality of the IMFs based on EMD is not guaranteed theoretically. For example, there are two Stokian waves each having many harmonics. If the frequency of one Stokian wave coincides with the frequency of a harmonic of the other, then the two waves are no longer orthogonal. However, the EMD can still separate the two Stokian waves as two IMFs. But the separated IMF components are not orthogonal. Fortunately, for most real time-varying dynamic system, the response signal consists of many components. The frequency of each component is time-dependent, but it does not coincide with the frequency of another component. Therefore, orthogonality is approximately satisfied in practical sense.

However, leakage occurs in the decomposition of signal using the EMD method. To check the orthogonality of the IMFs obtained from EMD, an index of orthogonality for any two components $y_f(t)$ and $y_g(t)$ is defined as

$$\mathrm{IO}_{fg} = \frac{1}{T} \sum_{t=0}^{T} \frac{|y_f(t) y_g(t)|}{y_f^2(t) + y_g^2(t)} \tag{2}$$

Leakage found in EMD method is typically less than 1%. For extremely short data, the leakage could be as high as 5%, which is comparable to that for a set of pure sinusoidal waves of the same data length [1].

Therefore, in most cases encountered, the leakage is small and the following condition is approximately satisfied

$$y_f(t) \cdot y_g(t) \approx 0 \quad (f \neq g) \tag{3}$$

indicating orthogonality for the pair of IMFs.

3. Identification algorithm based on forced vibration data

The equation of motion of an mdof LTV system due to forced excitation can be expressed as

$$\mathbf{M}(t)\ddot{\mathbf{y}}(t) + \mathbf{C}(t)\dot{\mathbf{y}}(t) + \mathbf{K}(t)\mathbf{y}(t) = \mathbf{f}(t) \tag{4}$$

in which $\mathbf{y}(t)$ is the displacement vector, $\mathbf{M}(t)$, $\mathbf{C}(t)$ and $\mathbf{K}(t)$ are $(n \times n)$ time-varying mass, damping and stiffness matrices, respectively, and $\mathbf{f}(t)$ is the excitation vector. The displacement vector $\mathbf{y}(t)$ can be decomposed using EMD method and expressed as the superposition of n IMFs as follows:

$$\mathbf{y}(t) = \sum_{j=1}^{n} y_j(t) \tag{5}$$

in which $y_j(t) = \{y_{1j}(t) \;\; y_{2j}(t) \;\; \cdots \;\; y_{nj}(t)\}^{\mathrm{T}}$ is the jth IMF extracted from the displacement vector using EMD method.

3.1. Hilbert transform

For the signal collected from the ith dof of a system, $y_{ij}(t)$ is the jth IMF, and the HT of this IMF is denoted by $\tilde{y}_{ij}(t)$ as

$$\tilde{y}_{ij}(t) = \mathrm{H}[y_{ij}(t)] = \frac{1}{\pi} P \int_{-\infty}^{+\infty} \frac{y_{ij}(\tau)}{t-\tau} \mathrm{d}\tau \tag{6}$$

where P is the Cauchy principal value. The analytical signal $Y_{ij}(t)$ of $y_{ij}(t)$ is expressed as

$$Y_{ij}(t) = y_{ij}(t) + \mathrm{j}\tilde{y}_{ij}(t) = A_{ij} \exp[\mathrm{j}\psi_{ij}(t)] \tag{7}$$

in which

$$y_{ij}(t) = A_{ij}(t) \cos \psi_{ij}(t)$$

$$A_{ij}(t) = \sqrt{y_{ij}^2(t) + \tilde{y}_{ij}^2(t)}$$

$$\psi_{ij}(t) = \arctan[\tilde{y}_{ij}(t)/y_{ij}(t)] \tag{8}$$

where $A_{ij}(t)$ is the instantaneous amplitude and $\psi_{ij}(t)$ is the instantaneous phase angle.

The instantaneous frequency $\omega_{ij}(t)$ is the time-derivative of the instantaneous phase, defined as

$$\omega_{ij}(t) = \dot{\psi}_{ij}(t) = \frac{y_{ij}(t)\dot{\tilde{y}}_{ij}(t) - \dot{y}_{ij}(t)\tilde{y}_{ij}(t)}{A_{ij}^2(t)} = \mathrm{Im}\left[\frac{\dot{Y}_{ij}(t)}{Y_{ij}(t)}\right] \tag{9}$$

The time-derivative of the instantaneous amplitude can be expressed as

$$\dot{A}_{ij}(t) = \frac{y_{ij}(t)\dot{y}_{ij}(t) + \tilde{y}_{ij}(t)\dot{\tilde{y}}_{ij}(t)}{A_{ij}(t)} = A_{ij}\,\mathrm{Re}\left[\frac{\dot{Y}_{ij}(t)}{Y_{ij}(t)}\right] \tag{10}$$

The first and second derivatives of $Y_{ij}(t)$ can be obtained from Eqs. (7) and (8) as

$$\dot{Y}_{ij}(t) = Y_{ij}(t)\left[\frac{\dot{A}_{ij}(t)}{A_{ij}(t)} + \mathrm{j}\omega_{ij}(t)\right] \tag{11}$$

$$\ddot{Y}_{ij}(t) = Y_{ij}(t)\left[\frac{\ddot{A}_{ij}(t)}{A_{ij}(t)} - \omega_{ij}^2(t) + \mathrm{j}\left(\frac{2\dot{A}_{ij}(t)\omega_{ij}(t)}{A_{ij}(t)} + \dot{\omega}_{ij}(t)\right)\right] \tag{12}$$

where

$$\dot{\omega}_{ij}(t) = \mathrm{Im}\left[\frac{\ddot{Y}_{ij}(t)}{Y_{ij}(t)}\right] - 2\frac{\dot{A}_{ij}(t)\omega_{ij}(t)}{A_{ij}(t)}, \quad \ddot{A}_{ij}(t) = A_{ij}(t)\left(\mathrm{Re}\left[\frac{\ddot{Y}_{ij}(t)}{Y_{ij}(t)}\right] + \omega_{ij}^2(t)\right) \tag{13}$$

3.2. mdof systems

According to the Bedrosian's theorem [14] on the HT of the product of two signals, we have

$$\mathrm{H}[\mathbf{M}(t)\ddot{\mathbf{y}}(t)] = \mathbf{M}(t)\mathrm{H}[\ddot{\mathbf{y}}(t)] = \mathbf{M}(t)\ddot{\tilde{\mathbf{y}}}(t)$$

$$\mathrm{H}[\mathbf{C}(t)\dot{\mathbf{y}}(t)] = \mathbf{C}(t)\mathrm{H}[\dot{\mathbf{y}}(t)] = \mathbf{C}(t)\dot{\tilde{\mathbf{y}}}(t)$$

$$\mathrm{H}[\mathbf{K}(t)\mathbf{y}(t)] = \mathbf{K}(t)\mathrm{H}[\mathbf{y}(t)] = \mathbf{K}(t)\tilde{\mathbf{y}}(t) \tag{14}$$

Apply HT to both sides of Eq. (4), and substituting Eq. (14), Eq. (4) becomes

$$\mathbf{M}(t)\ddot{\tilde{\mathbf{y}}}(t) + \mathbf{C}(t)\dot{\tilde{\mathbf{y}}}(t) + \mathbf{K}(t)\tilde{\mathbf{y}}(t) = \tilde{\mathbf{f}}(t) \tag{15}$$

Multiplying each term of Eq. (15) by j and adding it to the corresponding terms of Eq. (4), a differential equation on the analytic signal is obtained as

$$\mathbf{M}(t)\ddot{\mathbf{Y}}(t) + \mathbf{C}(t)\dot{\mathbf{Y}}(t) + \mathbf{K}(t)\mathbf{Y}(t) = \mathbf{F}(t) \tag{16}$$

in which $\mathbf{Y}(t) = \sum_{j=1}^{n}\mathbf{Y}_j(t)$, and $\mathbf{Y}_j(t)$ is the jth analytic signal, which can be written as

$$\mathbf{Y}_j(t) = \{Y_{1j}, Y_{2j}, \ldots, Y_{nj}\}^{\mathrm{T}} \tag{17}$$

Substituting Eqs. (11) and (12) for $\ddot{\mathbf{Y}}(t)$ and $\dot{\mathbf{Y}}(t)$ in Eq. (16), we have

$$\mathbf{M}(t)[\alpha^m]\mathbf{Y}(t) + \mathbf{C}(t)[\alpha^c]\mathbf{Y}(t) + \mathbf{K}(t)\mathbf{Y}(t) = \mathbf{F}(t) \tag{18}$$

where $[\alpha^m]$ and $[\alpha^c]$ are coefficients matrices, the element of which is denoted as

$$\alpha_{ij}^m = \left[\frac{\ddot{A}_{ij}(t)}{A_{ij}(t)} - \omega_{ij}^2(t)\right] + \mathrm{j}\left[\frac{2\dot{A}_{ij}(t)\omega_{ij}(t)}{A_{ij}(t)} + \dot{\omega}_{ij}(t)\right] \tag{19}$$

$$\alpha_{ij}^c = \frac{\dot{A}_{ij}(t)}{A_{ij}(t)} + \mathrm{j}\omega_{ij}(t) \tag{20}$$

For any two IMFs, $y_f(t)$ and $y_g(t)$, they are assumed to satisfy the orthogonal relationship $y_f(t)\cdot y_g(t) = 0$. And from the Bedrosian's theorem, it is easy to obtain

$$\mathbf{Y}_f(t)\cdot\mathbf{Y}_g(t) = 0 \tag{21}$$

Multiplying the two sides of Eq. (18) with $\mathbf{Y}_j^{\mathrm{T}}(t)$, we have

$$\mathbf{Y}_j^{\mathrm{T}}(t)\mathbf{M}(t)[\alpha^m]\mathbf{Y}_j(t) + \mathbf{Y}_j^{\mathrm{T}}(t)\mathbf{C}(t)[\alpha^c]\mathbf{Y}_j(t) + \mathbf{Y}_j^{\mathrm{T}}(t)\mathbf{K}(t)\mathbf{Y}_j(t) = \mathbf{Y}_j^{\mathrm{T}}(t)\mathbf{F}(t) \tag{22}$$

Assuming the mass matrix is known, Eq. (22) can be simplified and written in compact matrix notation using Eqs. (9), (10) and (13) as

$$\mathbf{P}^c\boldsymbol{\beta}^c + \mathbf{P}^k\boldsymbol{\beta}^k = \mathbf{P}^m \tag{23}$$

in which $\boldsymbol{\beta}^c = \{c_1 \ c_2 \ \cdots \ c_i \ \cdots \ c_n\}^{\mathrm{T}}$, $\boldsymbol{\beta}^k = \{k_1 \ k_2 \ \cdots \ k_i \ \cdots \ k_n\}^{\mathrm{T}}$, $\mathbf{P}^c$, $\mathbf{P}^k$ and $\mathbf{P}'^m$ are the coefficient matrices and vector. Elements in the jth row of these matrices are expressed as

$$\mathbf{P}_j^c = \begin{bmatrix} Y_{1j}\alpha_{1j}^c Y_{1j} \\ Y_{1j}(\alpha_{1j}^c Y_{1j} - \alpha_{2j}^c Y_{2j}) + Y_{2j}(\alpha_{2j}^c Y_{2j} - \alpha_{1j}^c Y_{1j}) \\ \vdots \\ Y_{i-1j}(\alpha_{i-1j}^c Y_{i-1j} - \alpha_{ij}^c Y_{ij}) + Y_{ij}(\alpha_{ij}^c Y_{ij} - \alpha_{i-1j}^c Y_{i-1j}) \\ \vdots \\ Y_{n-1j}(\alpha_{n-1j}^c Y_{n-1j} - \alpha_{nj}^c Y_{nj}) + Y_{nj}(\alpha_{nj}^c Y_{nj} - \alpha_{n-1j}^c Y_{n-1j}) \end{bmatrix}^{\mathrm{T}}$$

$$\mathbf{P}_j^k = \begin{bmatrix} Y_{1j}^2 \\ Y_{1j}(Y_{1j} - Y_{2j}) + Y_{2j}(Y_{2j} - Y_{1j}) \\ \vdots \\ Y_{i-1j}(Y_{i-1j} - Y_{ij}) + Y_{ij}(Y_{ij} - Y_{i-1j}) \\ \vdots \\ Y_{n-1j}(Y_{n-1j} - Y_{nj}) + Y_{nj}(Y_{nj} - Y_{n-1j}) \end{bmatrix}^{\mathrm{T}} \tag{24}$$

$$\mathbf{P}_j^m = \mathbf{Y}_j^{\mathrm{T}}\mathbf{F} - (Y_{1j}m_1\alpha_{1j}^m Y_{1j} + Y_{2j}m_2\alpha_{2j}^m Y_{2j} + Y_{ij}m_i\alpha_{ij}^m Y_{ij} + \cdots + Y_{nj}m_n\alpha_{nj}^m Y_{nj})$$

The complex equation (23) can be separated into two equations according to its real and imaginary parts, and they are subsequently assembled in the following form:

$$\begin{bmatrix} \mathrm{Re}(\mathbf{P}^c) & \mathrm{Re}(\mathbf{P}^k) \\ \mathrm{Im}(\mathbf{P}^c) & \mathrm{Im}(\mathbf{P}^k) \end{bmatrix} \begin{Bmatrix} \boldsymbol{\beta}^c \\ \boldsymbol{\beta}^k \end{Bmatrix} = \begin{Bmatrix} \mathrm{Re}(\mathbf{P}^m) \\ \mathrm{Im}(\mathbf{P}^m) \end{Bmatrix} \tag{25}$$

The above equation is a time-dependent identification equation for mdof systems. For an n dofs LTV system, Eq. (25) contains $2n$ time-varying equations. We can estimate the time-varying unknown system parameters at any time instant t by solving this identification equation.

3.3. sdof systems

For an sdof LTV system, the above identification algorithm can be simplified because the response data does not need to be decomposed using EMD method. The stiffness and damping coefficients can be written in the following explicit expressions as

$$c(t) = 2mh_0(t), \quad k(t) = m\omega_0^2(t) \tag{26}$$

in which $\omega_0(t)$ and $h_0(t)$ are the instantaneous undamped natural frequency and the instantaneous damping coefficient of the system, respectively, as

$$h_0(t) = \frac{\eta(t)}{2m\omega(t)} - \frac{\dot{A}(t)}{A(t)} - \frac{\dot{\omega}(t)}{2\omega(t)} \tag{27}$$

$$\omega_0^2(t) = \frac{k(t)}{m} = \omega^2(t) + \frac{\xi(t)}{m} - \frac{\eta(t)\dot{A}(t)}{m\omega(t)A(t)} - \frac{\ddot{A}(t)}{A(t)} + \frac{2\dot{A}^2(t)}{A^2(t)} + \frac{\dot{\omega}(t)\dot{A}(t)}{\omega(t)A(t)} \tag{28}$$

where $\omega(t)$, $\dot{A}(t)$, $\dot{\omega}(t)$ and $\ddot{A}(t)$ are the instantaneous coefficients, and $\xi(t)$ and $\eta(t)$ refer to the real and imaginary parts of impact excitation and response signal ratio according to the expression

$$\xi(t) = \mathrm{Re}\left[\frac{F(t)}{Y(t)}\right], \quad \eta(t) = \mathrm{Im}\left[\frac{F(t)}{Y(t)}\right] \tag{29}$$

4. Simulation studies

Several numerical examples on sdof and mdof LTV dynamic systems are studied in this section to illustrate the effectiveness and accuracy of the identification algorithm developed above. Three ideal cases of time variation are studied, which are smooth, abrupt and periodical variations, respectively. The identification of the varying system parameters is carried out for each of the systems using the forced vibration data. Results are also compared with those identified using free vibration data [13]. The response signals of the systems used in the identification are from the numerical solutions of the forced vibration differential equations using the Newton–Raphson method. The time interval between two computational steps is $\Delta t = T/N = \frac{10}{1024}$.

4.1. sdof systems

This section addresses the identification of time-varying stiffness and damping coefficients of a single dof mass–spring–damping dynamic system. The governing forced vibration equation of motion is given by

$$m\ddot{y}(t) + c(t)\dot{y}(t) + k(t)y(t) = f(t)$$

where m is the mass coefficient assumed as $m = 1.0\,\mathrm{kg}$, $c(t)$ and $k(t)$ are the time-dependent stiffness and damping coefficients, respectively, and $f(t)$ is the impact excitation force. It should be noted that the response is proportional to the excitation force in the present case where the LTV system parameters are assumed independent of the excitation.

Three time-varying cases are studied:

Case 1: A smooth change of stiffness and damping coefficients, i.e., $k(t) = 100\pi^2\,\mathrm{N/m}$, $c(t) = 0.7\,\mathrm{N\,s/m}$ for $t<2\,\mathrm{s}$; $k(t) = 100\pi^2-10\pi^2 t\,\mathrm{N/m}$, $c(t) = 0.7+0.15t\,\mathrm{N\,s/m}$ for $2\,\mathrm{s}\leqslant t\leqslant 4\,\mathrm{s}$ and $k(t) = 80\pi^2\,\mathrm{N/m}$, $c(t) = 1.0\,\mathrm{N\,s/m}$ for $t>4\,\mathrm{s}$.

Case 2: An abrupt change of stiffness coefficient, i.e., $k(t) = 100\pi^2\,\mathrm{N/m}$, $c(t) = 0.7\,\mathrm{N\,s/m}$ for $t<1.5\,\mathrm{s}$; $k(t) = 60\pi^2\,\mathrm{N/m}$, $c(t) = 0.7\,\mathrm{N\,s/m}$ for $1.5\,\mathrm{s}\leqslant t\leqslant 3.5\,\mathrm{s}$ and $k(t) = 80\pi^2\,\mathrm{N/m}$, $c(t) = 0.7\,\mathrm{N\,s/m}$ for $t>3.5\,\mathrm{s}$.

Case 3: A periodic change of stiffness, i.e., $k(t) = 100\pi^2-10\pi^2\sin(2\pi t)\,\mathrm{N/m}$ and $c(t) = 1.26\,\mathrm{N\,s/m}$.

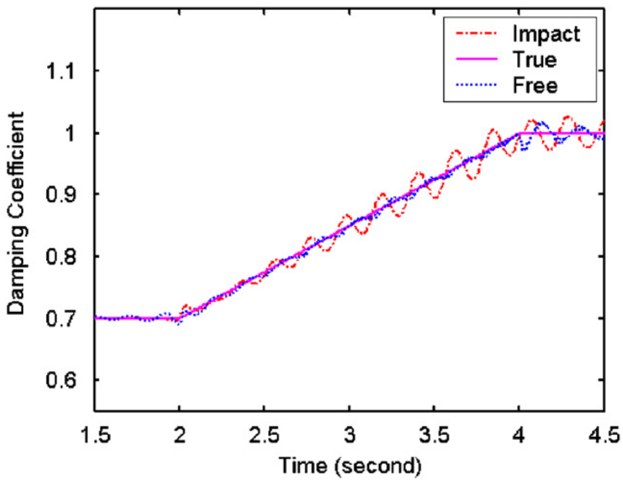

Fig. 1. sdof—Case 1: the estimated damping coefficient.

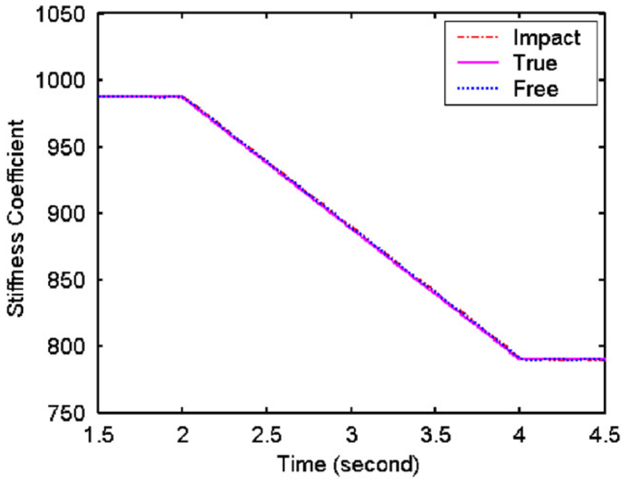

Fig. 2. sdof—Case 1: the estimated stiffness coefficient.

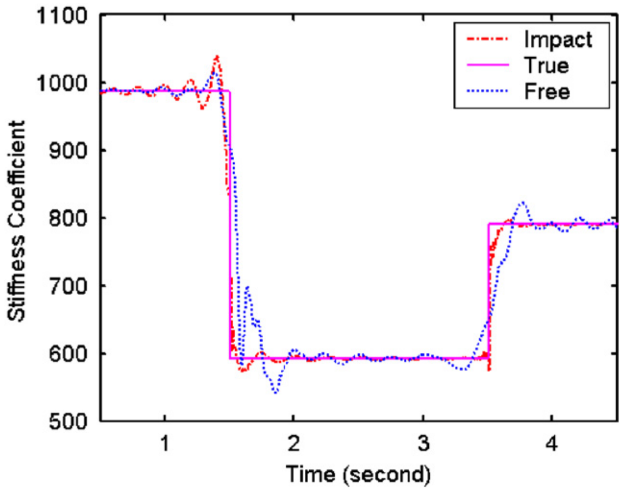

Fig. 3. sdof—Case 2: the estimated stiffness coefficient.

First the effectiveness and the robustness of the identification algorithm are studied for the case with a smooth change of stiffness and damping coefficients. Identified results are shown in Figs. 1 and 2. In all the figures, the dash-dot line denotes the identification result using forced vibration data, and the dotted line denotes the identification result using free vibration data [13]. The solid line denotes the true value. These three lines are named Impact, Free and True, respectively, in the legend of each figure. Fig. 1 gives a comparison of the identified damping coefficient with the true value. Fig. 2 shows a comparison of the identified stiffness coefficient with the true value. The identified damping and stiffness coefficients are found following the variation of the true value very closely.

The identified results for the two cases with abrupt change and periodic change of stiffness coefficient are shown in Figs. 3–5. Fig. 3 shows the identified results on the abrupt change of stiffness coefficient. Results illustrate that the estimated values closely track the abrupt changes of the true stiffness in the time duration, and there is large fluctuations before and after the time instances of abrupt change at $t = 1.5$ and 3.5 s. Similar tracking capability is also demonstrated in Fig. 4 on the periodically varying stiffness. The identified damping coefficient in Fig. 5 keeps track of the true value $c = 1.26$ in the whole duration of identification with small fluctuations.

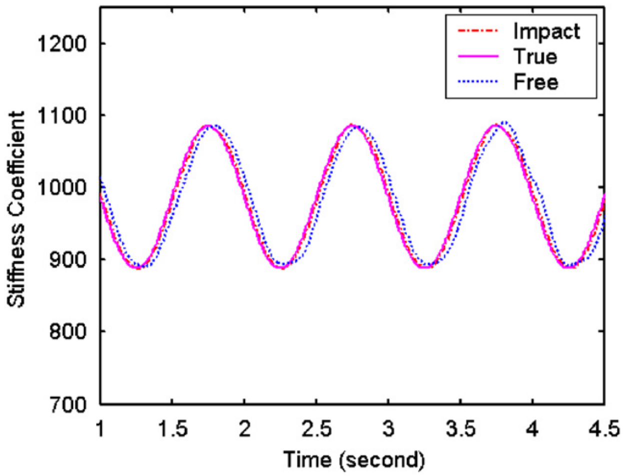

Fig. 4. sdof—Case 3: the estimated stiffness coefficient.

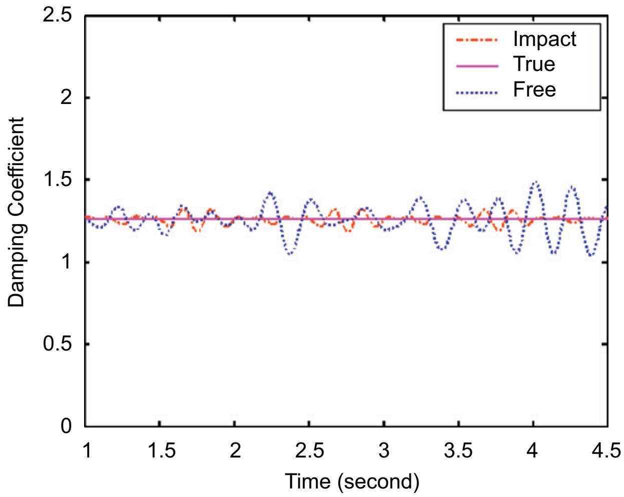

Fig. 5. sdof—Case 3: the estimated damping coefficient.

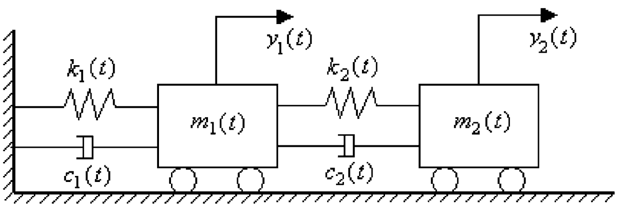

Fig. 6. Two dofs linear time-varying system.

4.2. Two degrees-of-freedom systems

The two dofs LTV system for numerical investigation is shown in Fig. 6. The two stiffness coefficients and the two damping coefficients are time-dependent, while the mass coefficients are assumed constant. In the following numerical examples, the mass coefficients are assumed constant at $m_1 = m_2 = 50\,\text{kg}$. The three cases of time variation, namely, the smoothly varying, periodically varying and abruptly varying systems, are studied to verify the ability and robustness of the identification algorithm for the mdof systems.

An impact excitation is applied to mass m_1. The vibration response signal is calculated based on the governing differential equations using the Newton–Raphson method. The identification algorithm for mdof systems is different from that for the sdof systems. For the latter case, the response signal can be directly analyzed using HT and then used to identify the time-varying parameters of the sdof system. However for the mdof systems, the response signal must be decomposed using EMD method to extract the IMF, which is suitable for analysis with the HT. The procedure for identification of an mdof system consists of the following steps:

- Step 1: Decompose the response signal (displacement, velocity or acceleration response) to extract all IMFs using EMD method according to steps listed under Section 2.
- Step 2: Analyze each IMF with HT and compute all time-dependent coefficients of the instantaneous amplitude, instantaneous frequency and their time-derivatives using Eqs. (9), (10) and (13).

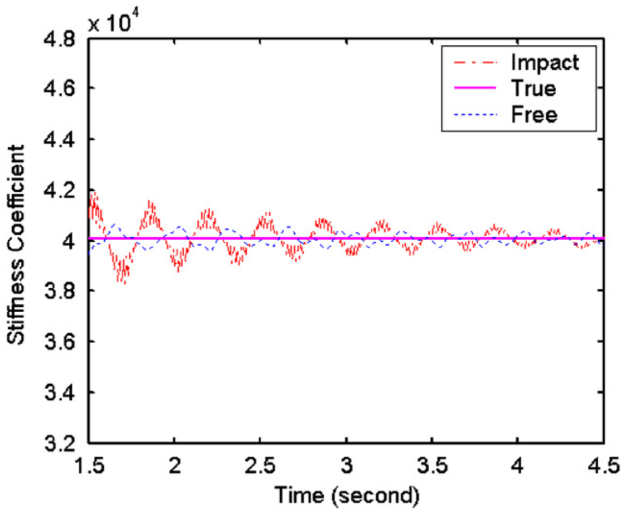

Fig. 7. mdof—Case 4: the estimated stiffness coefficient $k_1(t)$.

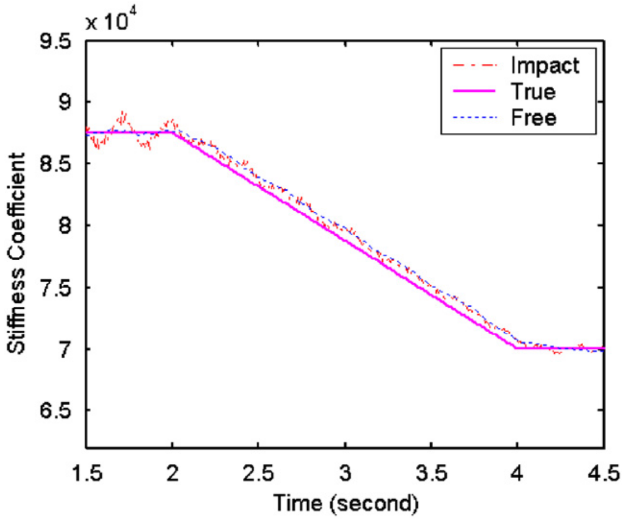

Fig. 8. mdof—Case 4: the estimated stiffness coefficient $k_2(t)$.

- Step 3: Calculate each element of the coefficient matrices $\mathbf{P}^c$, $\mathbf{P}^k$ and $\mathbf{P}^m$ according to Eq. (24), and form the identification equation (25).
- Step 4: Estimate the stiffness and damping coefficients from Eq. (25) for each time instant t.

The identification algorithm is developed based on the orthogonal relationship for any two IMFs. The degree of orthogonality of any two IMFs will affect the identification results of the mdof systems, and it will be discussed in the following section.

The parameters of the three time-varying systems are:

Case 4: An LTV system with smoothly varying stiffness. The stiffness coefficients are given by $k_1 = 40\,053$ N/m, $k_2 = 87\,552$ N/m when $t < 2$ s; $k_1 = 40\,053$ N/m, $k_2 = 87\,552 - 8755.2t$ N/m when $2\,\mathrm{s} \leqslant t \leqslant 4\,\mathrm{s}$ and $k_1 = 40\,053$ N/m, $k_2 = 70\,042$ N/m when $t > 4$ s. The damping coefficients are assumed as $c_1 = 30$ N s/m, $c_2 = 0.0$ N s/m.

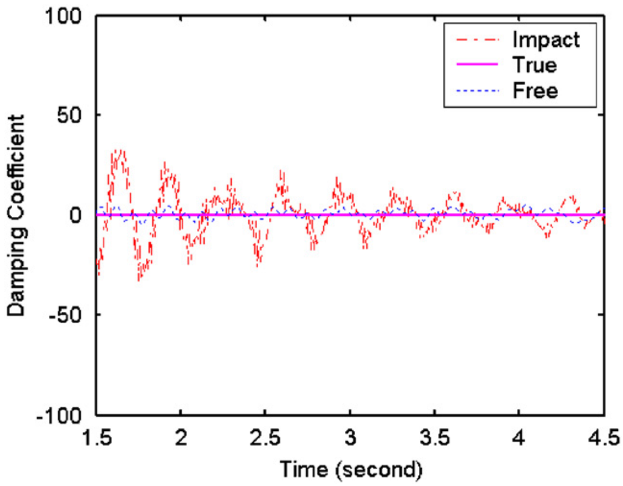

Fig. 9. mdof—Case 4: the estimated damping coefficient $c_2(t)$.

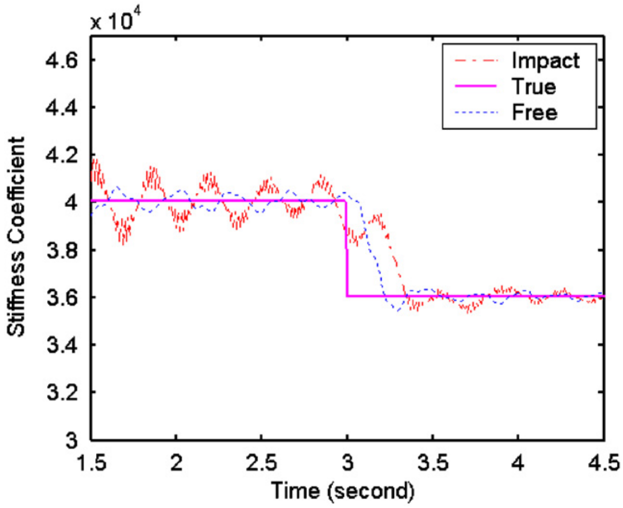

Fig. 10. mdof—Case 5: the estimated stiffness coefficient $k_1(t)$.

Case 5: An LTV system with abruptly varying stiffness. The stiffness coefficients are given by $k_1 = 40\,053\,\mathrm{N/m}$, $k_2 = 87\,552\,\mathrm{N/m}$ when $t \leqslant 3\,\mathrm{s}$ and $k_1 = 36\,048\,\mathrm{N/m}$, $k_2 = 70\,042\,\mathrm{N/m}$ when $t > 3\,\mathrm{s}$. The damping coefficients are assumed constant as $c_1 = 30\,\mathrm{N\,s/m}$, $c_2 = 0.0\,\mathrm{N\,s/m}$.

Case 6: An LTV system with periodically varying stiffness. The stiffness coefficients are given by $k_1 = 40\,053\,\mathrm{N/m}$, $k_2 = 87\,552\,\mathrm{N/m}$ when $t < 2\,\mathrm{s}$ and $k_1 = 40\,053 - 4005.3\,\sin(\pi t)\,\mathrm{N/m}$, $k_2 = 87\,552\,\mathrm{N/m}$ when $t \geqslant 2\,\mathrm{s}$. The damping coefficients are assumed constant as $c_1 = 30\,\mathrm{N\,s/m}$, $c_2 = 0.0\,\mathrm{N\,s/m}$.

Based on the identification algorithm proposed in this paper and in Ref. [13], the stiffness and damping coefficients for the above cases are estimated using forced vibration data and free vibration data. All identified results are compared with the true value. Case 4 is investigated to demonstrate the capability of the identification algorithm to track the smooth variation of the system, and the results are shown in Figs. 7–9. Figs. 7–9 show the identified stiffnesses $k_1(t)$, $k_2(t)$ and the damping coefficient $c_2(t)$, respectively. Case 5 is studied to further illustrate the ability of the identification method for tracking an abrupt variation in the system. The comparison of the estimated stiffnesses $k_1(t)$, $k_2(t)$ and the damping coefficients $c_1(t)$, $c_2(t)$ with the corresponding true value are shown in Figs. 10–13, respectively. The performance of the identification

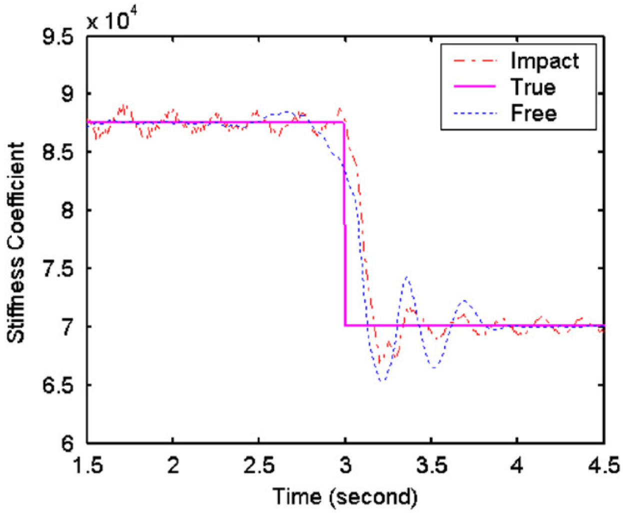

Fig. 11. mdof—Case 5: the estimated stiffness coefficient $k_2(t)$.

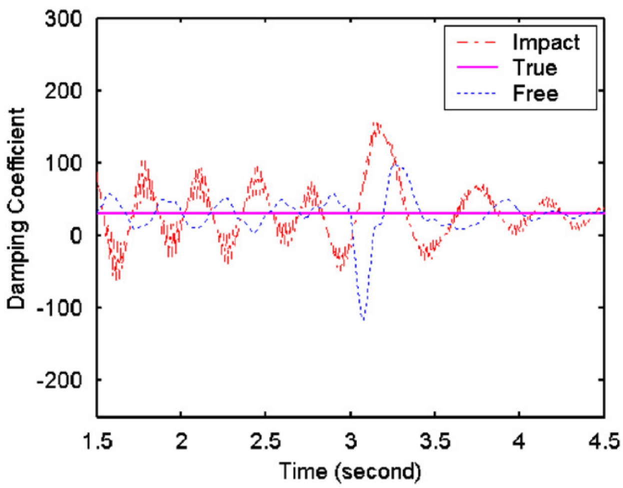

Fig. 12. mdof—Case 5: the estimated damping coefficient $c_1(t)$.

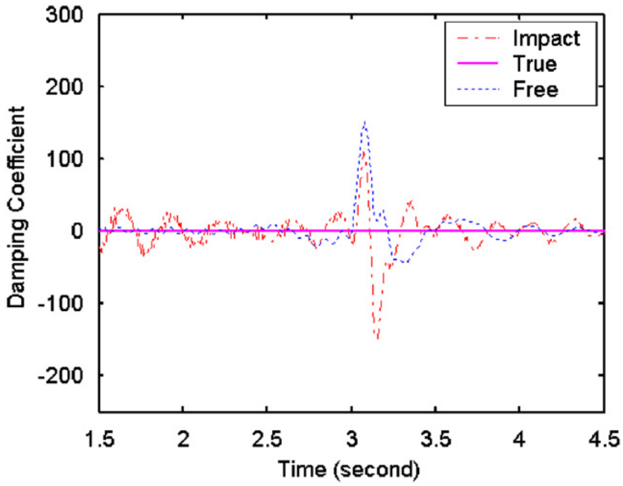

Fig. 13. mdof—Case 5: the estimated damping coefficient $c_2(t)$.

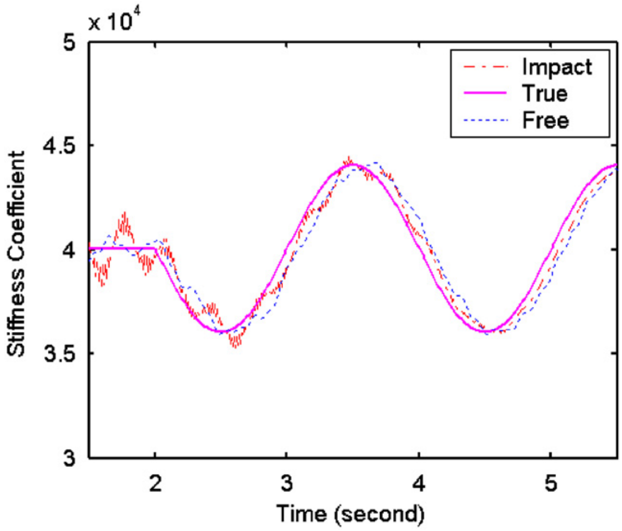

Fig. 14. mdof—Case 6: the estimated stiffness coefficient $k_1(t)$.

algorithm to track the periodic variation is investigated using Case 6. Figs. 14 and 15 illustrate the comparison of the estimated stiffness $k_1(t)$ and $k_2(t)$ with the corresponding true value, and Fig. 16 shows the comparison of the identified damping coefficient $c_2(t)$ with the true value $c_2 = 0.0\,\mathrm{N\,s/m}$.

The identified results are accurate and they fluctuate close to the true values. The error of identification in the parameters at the instance of abrupt change for Case 5 is large, but the identified values fluctuate around the true values in the remaining time duration. The proposed algorithm has good capability of tracking the variations of the system parameters of an mdof even for the case with abrupt changes in the parameters.

4.3. A four-story shear-beam building model

A four-story shear-beam building model is shown in Fig. 17. The mass coefficients are assumed constant at $m_1 = m_2 = m_3 = m_4 = 10\,\mathrm{kg}$. The stiffness and damping coefficients are time-dependent. The initial four stiffness coefficients and damping coefficients are $k_1 = 116\,000$, $k_2 = 96\,000$, $k_3 = 76\,000$, $k_4 = 56\,000\,\mathrm{N/m}$, and $c_1 = 34.8$, $c_2 = 28.8$, $c_3 = 28.8$, $c_4 = 28.8\,\mathrm{N\,s/m}$, respectively.

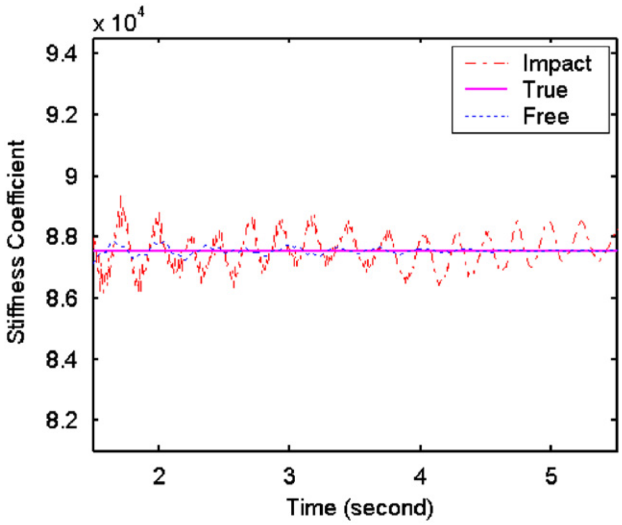

Fig. 15. mdof—Case 6: the estimated stiffness coefficient $k_2(t)$.

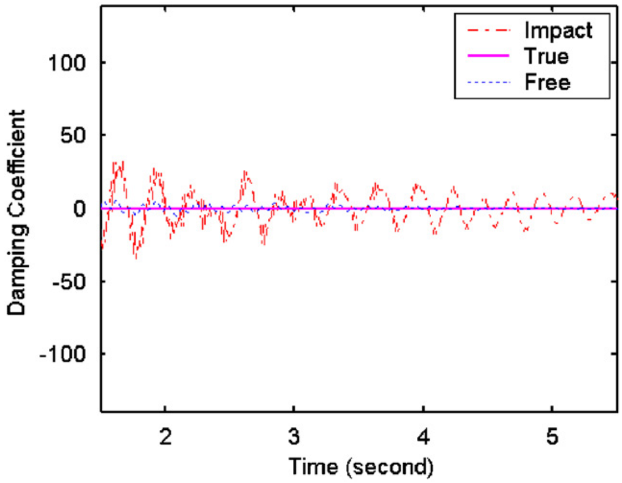

Fig. 16. mdof—Case 6: the estimated damping coefficient $c_2(t)$.

Three time-varying cases, i.e., the smoothly, periodically and abruptly varying scenarios, are studied to verify the ability and robustness of the identification algorithm.

Case 7: An LTV system with smoothly varying stiffness. The stiffness coefficients are given by $k_1(t) = 116\,000$, $k_3(t) = 76\,000\,\text{N/m}$ when $t < 2\,\text{s}$; $k_1(t) = 116\,000 - 7600(t-2)$, $k_3 = 76\,000 - 5000(t-2)$ N/m when $2\,\text{s} \leqslant t \leqslant 5\,\text{s}$ and $k_1(t) = 93\,200$, $k_3(t) = 61\,000\,\text{N/m}$ when $t > 5\,\text{s}$. The other two stiffness coefficients are assumed as constant at their initial values.

Case 8: An LTV system with abruptly varying stiffness. The stiffness coefficients are given by $k_1(t) = 116\,000\,\text{N/m}$ when $t \leqslant 2\,\text{s}$ and $k_1 = 81\,200\,\text{N/m}$ when $t > 2\,\text{s}$. The other stiffness coefficients are assumed as constant at their initial values.

Case 9: An LTV system with periodically varying stiffness. The stiffness coefficients are given by $k_1(t) = 116\,000$, $k_2(t) = 96\,000\,\text{N/m}$ when $t < 2\,\text{s}$ and $k_1(t) = 116\,000 - 25\,000\,\sin[2\pi(t-2)]$, $k_2(t) = 96\,000 - 20\,000\,\sin[2\pi(t-2)]\,\text{N/m}$ when $t \geqslant 2\,\text{s}$. The other stiffness coefficients are assumed as constant at their initial values.

An impact excitation is applied to masses m_2 and m_4 of the shear-beam building model. The vibration response signal is calculated based on the governing differential equations using the Newton–Raphson method. The identification procedure has been described in Section 4.2 in four steps.

The stiffness and damping coefficients for the above cases are identified using response data under impact excitation and free vibration data. All identified results are compared with the true values. The dash-dot line denotes the identification result using forced vibration data, and the dotted line denotes the identification result using free vibration data. The solid line denotes the true value. These three lines are named Impact, Free and True, respectively, in the legend of each figure. Case 7 shows the ability of the identification method for tracking the smooth variation of the system. Fig. 18 shows the comparison of the identified stiffness coefficient $k_1(t)$ using the third IMF. The stiffness coefficient $k_3(t)$ identified using the fourth IMF is shown in Fig. 19. There is a small time delay in the change of the stiffness similar to the observation on the results for Case 4 in Fig. 8. Case 8 is investigated to demonstrate the capability of the identification algorithm for tracking an abrupt variation in the system. The comparison of the stiffness coefficients $k_1(t)$ estimated using all IMF extracted from impact and free response data with the corresponding true value are shown in Fig. 20.

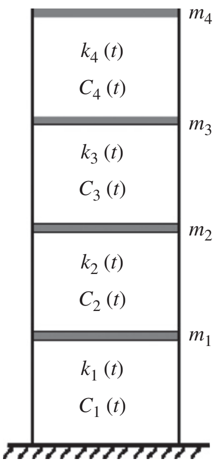

Fig. 17. A four-story shear-beam building model.

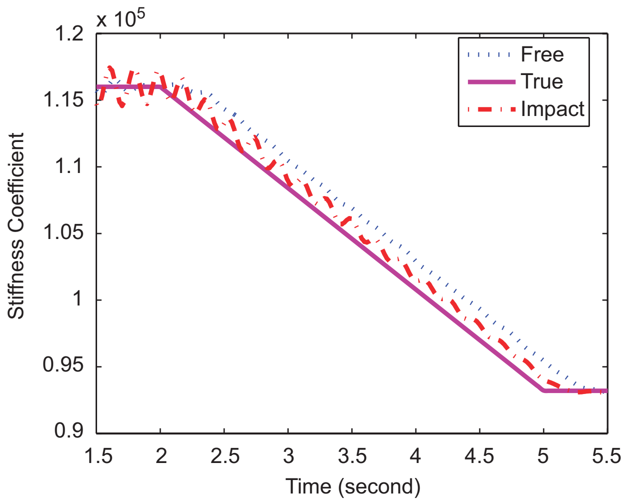

Fig. 18. mdof—Case 7: the estimated stiffness coefficient $k_1(t)$.

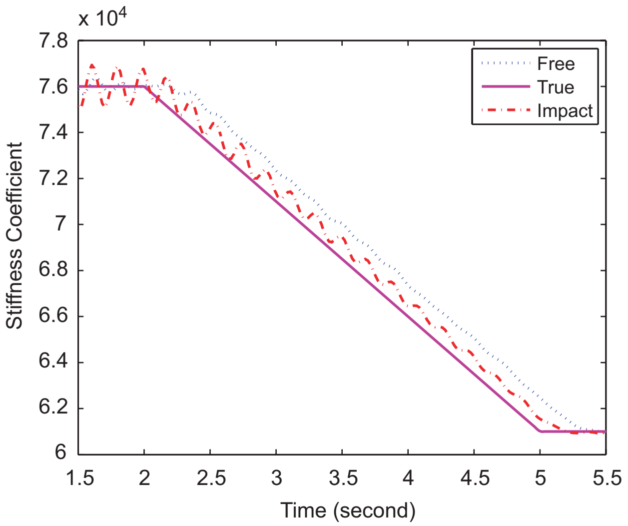

Fig. 19. mdof—Case 7: the estimated stiffness coefficient $k_3(t)$.

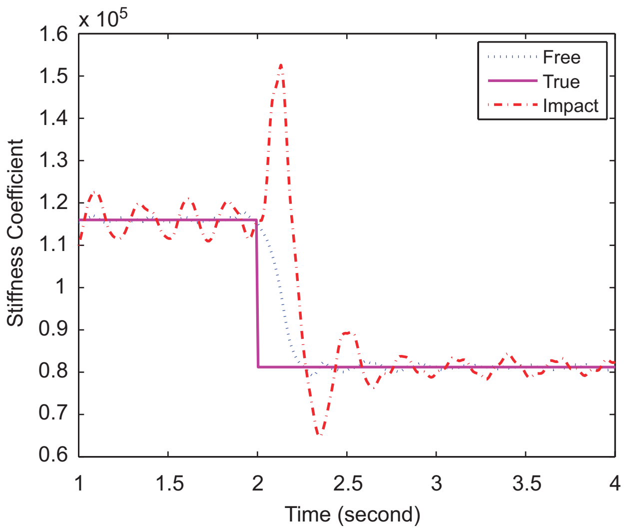

Fig. 20. mdof—Case 8: the estimated stiffness coefficient $k_1(t)$.

The fluctuation at the time instance of stiffness change is larger from the impact induced response than the free vibration response, but the identified results varies gently around the true value in the other time instances. The performance of the identification algorithm to track the periodic variation is investigated using Case 9. Figs. 21 and 22 illustrate the comparison of the stiffness $k_1(t)$ estimated using first IMF and four IMFs, respectively, with the corresponding true value. The comparison of the stiffness $k_2(t)$ estimated using all IMFs with the corresponding true value is shown in Fig. 23. These figures show that using either a single or multiple IMFs can yield good results on the stiffness change. The variation of the damping coefficients are similar to those shown for the two dofs system and are not shown here.

The stiffness coefficients identified using free response data are more accurate than those identified using the impact-induced response data. However, all estimated stiffness coefficients fluctuate close to the

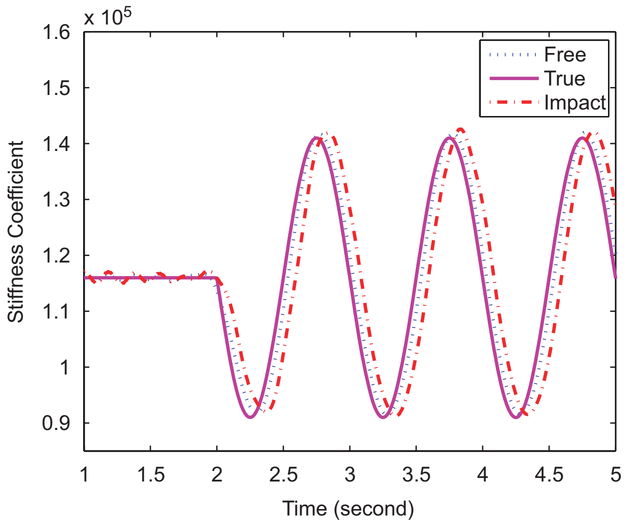

Fig. 21. mdof—Case 9: the estimated stiffness coefficient $k_1(t)$.

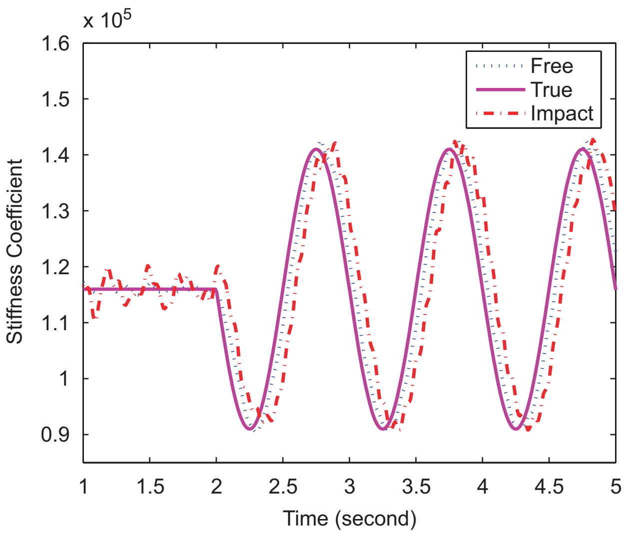

Fig. 22. mdof—Case 9: the estimated stiffness coefficient $k_1(t)$.

corresponding true values. The error of identified stiffness coefficients is small except at the time instance of abrupt change for Case 8. Results show that the proposed algorithm has good capability of tracking the variations of the system parameters of an mdof even for the case with abrupt changes in the parameters.

4.4. Orthogonality of IMFs

It is noted that the identified results for mdof systems are less accurate than those for sdof systems, and are also less accurate than results identified using free vibration data. It is suspected that the assumption of orthogonality between any two IMF in Eq. (3) in the development of the presented identification algorithm leads to this error. A study is made on the orthogonality index of any two IMFs for the three types of mdofs systems, and they are given in Table 1. Each index is calculated from Eq. (3), and the IMFs are decomposed

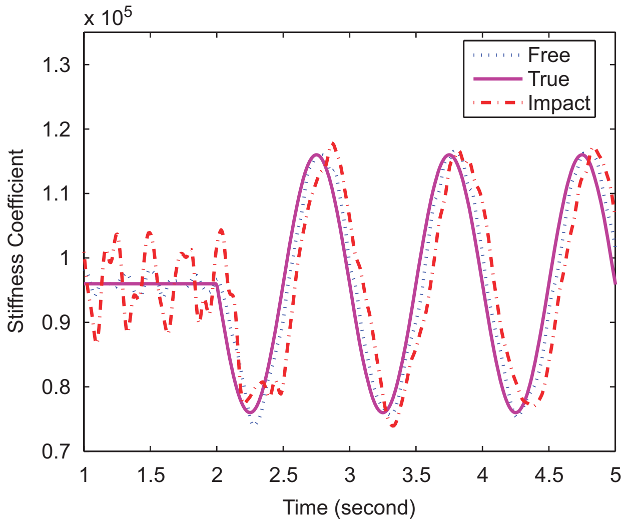

Fig. 23. mdof—Case 9: the estimated stiffness coefficient $k_2(t)$.

Table 1
Orthogonal index values of three ideal cases for mdof systems.

Response signal	Case 4 (%)	Case 5 (%)	Case 6 (%)
Displacement response	1.10	1.15	1.09
Velocity response	1.21	1.27	1.21
Acceleration response	1.00	1.07	0.98

from the response signal of displacement, velocity and accelerate response signals. It is observed that all the orthogonal indices are small around 1%, but they are not equal to zero. This shows that the decomposed IMFs are not completely orthogonal, and this type of error in the orthogonality property would be a significant source of error affecting the accuracy of the identification results.

5. Conclusions

An identification algorithm for linear time-varying (LTV) mdof dynamic system has been developed based on the Hilbert transform and the empirical mode decomposition method using forced vibration response time histories. The orthogonality of any two intrinsic mode functions extracted from the response signal is studied and discussed. The identification algorithm is applied to three ideal cases, namely, the smoothly varying, periodically varying and abruptly varying stiffness and damping of the LTV system, to investigate the capability of tracking these variations. All estimated results are compared with those identified using free vibration response based on the identification approach in Ref. [13]. It is noted that the lack of complete orthogonality of any two IMFs affects the accuracy of the identification results. However, simulation results show that the proposed identification algorithm is still effective and robust to identify the time-dependent stiffness and damping coefficients of both the single degree-of-freedom system and the multiple degrees-of-freedom system.

Acknowledgment

This research is supported by the National Natural Science Foundation of China through Grant no. 10772076, a research grant from the Hong Kong Polytechnic University Grant no. G-YX26 and the National Science Foundation of Jiang Su Province through Grant no. BK2006520.

References

[1] N.E. Huang, Z. Shen, S.R. Long, M.C. Wu, H.H. Shih, The empirical mode decomposition and Hilbert spectrum for nonlinear and nonstationary time series analysis, *Proceedings of the Royal Society of London—Series A* 454 (1998) 903–995.

[2] K. Liu, Identification of linear time-varying systems, *Journal of Sound and Vibration* 206 (4) (1997) 487–505.

[3] K. Liu, Extension of modal analysis to linear time-varying systems, *Journal of Sound and Vibration* 226 (1) (1999) 149–167.

[4] K. Liu, L. Deng, Experimental verification of an algorithm for identification of linear time-varying systems, *Journal of Sound and Vibration* 279 (2005) 1170–1180.

[5] Z.Y. Shi, S.S. Law, H.N. Li, Subspace-based identification of linear time-varying system, *AIAA Journal* 45 (8) (2007) 2042–2050.

[6] R. Ghanem, F. Romeo, A wavelet-based approach for the identification of linear time-varying dynamical systems, *Journal of Sound and Vibration* 234 (4) (2000) 555–576.

[7] H.P. Zhao, J. Bentsman, Biorthogonal wavelet based identification of fast linear time-varying systems—part I: system representations, *Journal of Dynamic Systems, Measurement and Control* 123 (4) (2001) 585–592.

[8] E.B. Kosmatopolous, A.W. Smyth, S.F. Masri, A.G. Chassiakos, Robust adaptive neural estimation of restoring forces in nonlinear structures, *Journal of Applied Mechanics* 68 (6) (2001) 880–893.

[9] A.W. Smyth, S.F. Masri, E.B. Kosmatopoulos, A.G. Chassiakos, T.K. Caughey, Development of adaptive modeling techniques for non-linear hysteretic systems, *International Journal of Non-Linear Mechanics* 37 (8) (2002) 1435–1451.

[10] J.N. Yang, S. Lin, Identification of parametric variations of structures based on least square estimation and adaptive tracking technique, *Journal of Engineering Mechanics—ASCE* 131 (3) (2005) 290–298.

[11] M. Feldman, Non-linear system vibration analysis using Hilbert transform—I: free vibration analysis method FREEVIB, *Mechanical Systems and Signal Processing* 8 (2) (1994) 119–127.

[12] M. Feldman, Non-linear system vibration analysis using Hilbert transform—II: forced vibration analysis method FORCEVIB, *Mechanical Systems and Signal Processing* 8 (3) (1994) 309–318.

[13] Z.Y. Shi, S.S. Law, Identification of linear time-varying dynamical system using Hilbert transform and EMD method, *Journal of Applied Mechanics* 74 (2) (2007) 223–230.

[14] L.H. Stefan, *Hilbert Transform in Signal Processing*, Artech House Inc., Norwood, MA, 1996.